ACS OMEGA

http://pubs.acs.org/journal/acsodf

Article

Colorimetric Sensing of Volatile Organic Compounds Produced from Heated Cooking Oils

Emer Duffy,* Emme Cauven, and Aoife Morrin*

Cite This: *ACS Omega* 2021, 6, 7394−7401

Read Online

ACCESS | Metrics & More | Article Recommendations | Supporting Information

ABSTRACT: Measurement of cooking-associated air pollution indoors is an integral part of exposure monitoring and human health risk assessment. There is a need for easy to use, fast, and economical detection systems to quantify the various emissions from different sources in the home. Addressing this challenge, a colorimetric sensor array (CSA) is reported as a new method to characterize volatile organic compounds produced from cooking, a major contributor to indoor air pollution. The sensor array is composed of pH indicators and aniline dyes from classical spot tests, which enabled molecular recognition of a variety of aldehydes, ketones, and carboxylic acids as demonstrated by hierarchical clustering and principal component analyses. To demonstrate the concept, these CSAs were employed for differentiation of emissions from heated cooking oils (sunflower, rapeseed, olive, and groundnut oils). Sensor results were validated by gas chromatography−mass spectrometry analysis, highlighting the potential of the sensor array for evaluating cooking emissions as a source of indoor air pollution.

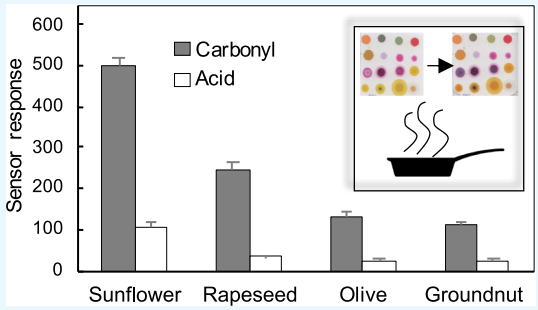

INTRODUCTION

Cooking is an important source of indoor air pollution as it emits a wide range of harmful pollutants that include volatile organic compounds (VOCs), polycyclic aromatic hydrocarbons, and particulate matter.[1] Cooking emissions vary depending on the type of food material, edible oils, and the cooking style used.[2] Frying is among the highest emitting types of cooking[3,4] in addition to other high-temperature cooking methods (e.g., grilling over open flames) and cooking foods rich in protein or fat.[5−7] Numerous reports indicate that the emissions produced from heating edible oils to high temperatures exhibit mutagenicity,[8,9] and fumes from frying at high temperatures have been classified into group 2A (probable human carcinogen) by the International Agency of Research on Cancer.[10]

The main volatile compounds generated during edible oil degradation are aldehydes, ketones, hydrocarbons, alcohols, and carboxylic acids.[11] Volatile aldehydes form the major component of cooking oil emissions,[12] and this group of compounds is of particular concern in relation to carcinogenicity, especially acrolein[13,14] and *t,t*-2,4-decadienal.[15,16] Volatile aldehydes are also irritants of the eyes, skin, and mucous membranes of the respiratory tract, making them emissions of concern to individuals who routinely fry with oil at home, in addition to those working in occupational cooking settings. Commercial kitchens typically have ventilation systems in place; however, these are often lacking (or not utilized) in domestic situations. Moreover, air pollution generated during cooking events has been shown to persist in the home for many hours. For instance, Seaman et al. found that the indoor half-life of acrolein produced from cooking was up to 14.4 h.[14]

Measurement of cooking-associated air pollution indoors is an integral part of exposure monitoring and human health risk assessment. In-field monitoring of target VOCs should be based on an easy to use, fast, and economical detection system to specify the roles of various emission sources (e.g., cooking technique, edible oils, and food type). The detection of VOCs indoors generally relies on high-end instrumentation such as PTR-TOF-MS[17,18] or off-line measurements like gas chromatography−mass spectrometry (GC−MS)[19] in combination with a preconcentration step. These traditional measurement approaches provide high quality data, but their high associated costs and low deployment density limit the scale of air pollution studies, making it difficult to represent the exposure pattern of a population. Low-cost sensors may enhance indoor air pollution monitoring capabilities by enabling higher density deployment and collection of more representative exposure data in a variety of settings. Numerous sensor systems have been proposed for monitoring VOCs, including quartz crystal microbalances,[20] electrochemical resistors,[21] optical sensors,[22,23] and colorimetric sensor arrays.[24−26]

Received: November 21, 2020
Accepted: January 19, 2021
Published: March 8, 2021

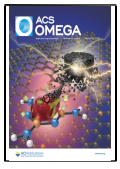

https://dx.doi.org/10.1021/acsomega.0c05667
ACS Omega 2021, 6, 7394−7401

The colorimetric sensor array (CSA) method for detection of VOCs was first proposed by Rakow and Suslick.[27] The CSA approach is advantageous for discrimination of complex mixtures based on strong chemical interactions between a sensor and analyte, rather than relying on nonspecific interactions (e.g., physisorption) that solely depend on the physical traits of the analyte or on the surface features of the sensor.[28] A variety of sensing systems have since been developed and have demonstrated a strong capability of detecting diverse VOCs in air samples[29−34] making them a promising approach for monitoring indoor air pollution. The use of optical detection in combination with CSAs is particularly advantageous for indoor air monitoring, due to its high sensitivity and the associated convenient instrumentation (e.g., digital camera or comparison to color reference strips), making it highly suitable for deployment in residential and commercial settings alike.

The aim of the present study was to develop a CSA method to characterize VOC emissions from heated cooking oils. The array was designed to target VOCs commonly found in cooking oil emissions (aldehydes, ketones, and carboxylic acids) by incorporating pararosaniline, 4,4-azodianiline, and pH indicators as sensing materials. The potential of the CSA to discriminate between key volatiles was investigated using a set of standard analytes with hierarchical cluster analysis and principal component analysis. The potential of the CSA to characterize emissions from heated cooking oils was investigated by comparing the GC−MS and CSA data using linear regression.

RESULTS AND DISCUSSION

Characterizing Sensor Response to Standard Analytes. The CSA was designed to show a selective response to volatile organic acids, aldehydes, and ketones by incorporating pH sensors (targeting acids) and amine-containing sensors (targeting nucleophilic addition to a carbonyl group by an amine in the formation of an imine) to yield different visible wavelength absorbance bands. Digital imaging of sensor arrays before and after exposure enabled quantitative measurement of RGB color changes to generate a multidimensional response referred to as a difference map. Each difference map encompasses ΔR, ΔG, and ΔB values and is unique to a particular analytes' interactions with the sensor elements. In order to understand the capability of the array to discriminate between aldehydes, acids, and other compounds, sensor response to a set of 14 standard analytes was tested. The difference maps obtained are shown in Figure 1. The sensor array responses provided visually distinguishable patterns for each compound under investigation. Distinct color changes were observed for the amine-containing sensors in the presence of aldehydes including the alkanals, alkenals, and alkadienals under investigation. In general, the pararosaniline sensors showed a change in color from pink to purple, and the 4,4′-azodianiline sensors changed from yellow to orange/brown in the presence of aldehyde vapors (Figure S4). These sensors changed to a lesser extent in response to ketones like acetone and geranyl acetone.

Sensors 1, 2, 3, and 5 showed the strongest interaction with the acids investigated, particularly with the shorter chain acids (formic and acetic acid). The intensity of the color change is primarily dependent on the reactivity of the analyte, including the electrophilicity of carbonyl groups present during the nucleophilic addition for sensors 7−16. Aliphatic aldehydes

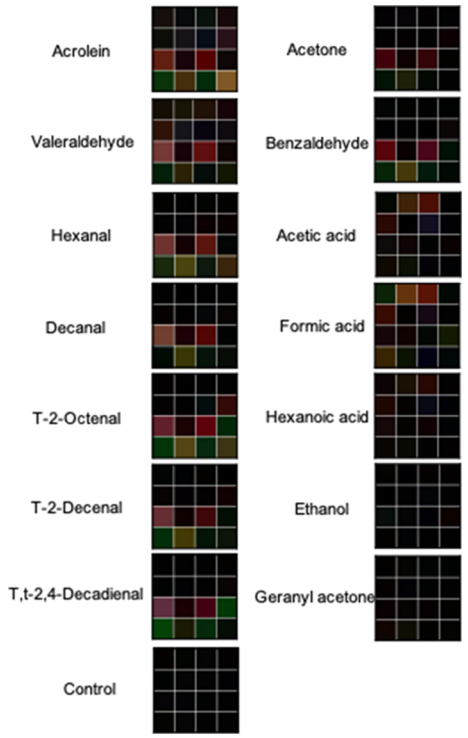

Figure 1. Difference maps showing the change in color (ΔRGB) for each sensor on the array after exposure to standard vapors.

(e.g., hexanal) are more responsive than aromatic (e.g., benzaldehyde), and aldehydes (e.g., acrolein) are more responsive than ketones (e.g., acetone). The color change also gradually lessens as the length of the analyte's carbon chain (and its vapor pressure) decreases. Very little response was observed for the amine-containing sensors in the presence of acids. A small color change in the presence of formic acid and acetic acid was observed, potentially due to the presence of the carboxylic acid functional group; however, the lower electrophilicity of the acids produced little response in this group of sensors in comparison to the aldehydes. The sensor array was exposed to ethanol and background air inside the test chamber to test for interferences, and very low sensor responses were observed in both cases (as shown in Figure 1). The sensor array was also exposed to different conditions of humidity, and very little response was observed owing to the use of hydrophobic formulations in the array, as shown in Figure S5.

Hierarchical clustering analysis (HCA) and principal component analysis (PCA) were performed on the dataset (comprising 240 ΔE values, for each sensor on the array in response to standard analyte vapors, where ΔE was calculated using eq 1) to understand the capability of the sensor array to discriminate between aldehydes, acids, and other compounds. The HCA dendrogram in Figure 2 shows successful discrimination between the analytes under investigation. The x axis of the dendrogram represents the distance or dissimilarity between the clusters, and each leaf corresponds to one analyte. The samples were clustered into four categories, which corresponded to the analytes' structural and chemical properties. Branches that are close to the same height on the x axis are similar to each other, such as ethanol and acetone, which showed similarly low sensor responses. Formic acid and acetic acid were less similar in comparison

https://dx.doi.org/10.1021/acsomega.0c05667
ACS Omega 2021, 6, 7394−7401

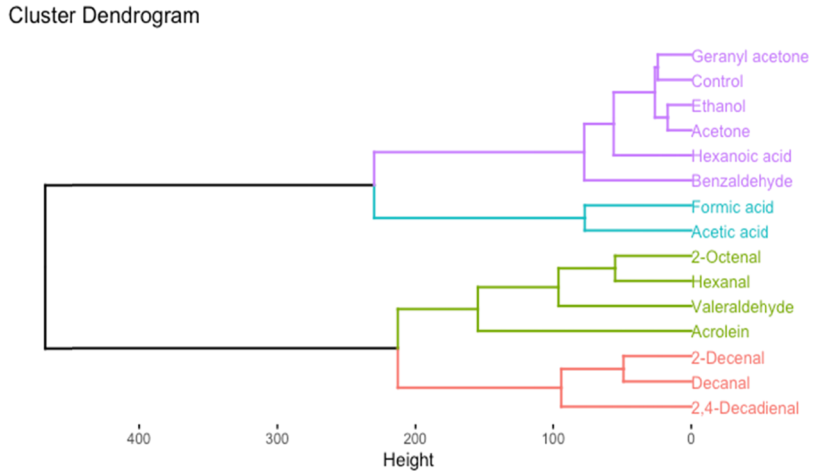

Figure 2. Dendrogram from hierarchical clustering analysis (HCA) of sensor array response to standard analytes and air control.

(i.e., the branches fuse at a higher point on the *x* axis) due to their strong characteristic interactions with sensors S1−S5 (as seen in Figure 1 and Figure S4). The aliphatic aldehydes were clustered into two categories according to their chain length (C_3-C_8 and C_{10}) with distinct distances evident between each analyte. These clusters included alkanals, alkenals, and alkadienals but excluded the aromatic aldehyde (benzaldehyde), which produced a lower sensor response. Benzaldehyde was clustered with the other less reactive (e.g., acetone and ethanol) and less volatile (e.g., hexanoic acid and geranyl acetone) analytes, in addition to the control sample, for which similar low sensor responses were observed.

PCA also classified the analytes into four groups, similar to the clusters observed in Figure 2. Figure S6 shows the scores plot from PCA where the aliphatic aldehydes were separated from the other analytes with positive scores on principal component 1 (PC1). Formic acid, acetic acid, hexanoic acid, benzaldehyde, and the other compounds showed negative scores on PC1. The aliphatic aldehydes were separated on PC1 based on their strong interaction with the amine-containing sensors. Figure S7 shows that sensors 8−16 made an important contribution to the ability of the CSA to discriminate between aliphatic aldehydes and other analytes, and a higher score on PC1 indicates a stronger interaction between an analyte and these sensors (as measured by the intensity of the sensor response). The acids were differentiated from the other compounds on PC2 based on their strong interaction with the acid sensors (Figure S6). Figure S8 shows that sensors 1−5 and sensor 7 made an important contribution to the ability of the CSA to discriminate within groups of acids and aliphatic aldehydes based on analyte reactivity, where a higher score on PC2 indicates a stronger interaction between an analyte and these sensors. The contribution of all variables (sensors) to PC 1 and 2 is also shown in a correlation plot (Figure S9), which highlights the important role played by the majority of sensors in distinguishing between the acids, aldehydes, and other compounds tested. A low contribution was observed for sensors 6 and 12; therefore, these sensors may be nonessential for this particular analysis. However, given the complexity of the target matrix (cooking emissions), all sensors were retained in the array. The results obtained from HCA and PCA highlight the capability of the sensor array to successfully discriminate between structurally similar aliphatic aldehydes, short chain acids, and other compounds. These results are limited to the analyte concentration studied, as different sensors may have different responses at varying concentrations of an analyte.

The sensor array was subsequently applied to a quantitative analysis of different concentrations of a single aldehyde (acrolein) and acid (acetic acid). The acid sensors showed a visible color change in the presence of acetic acid vapor (Figure 3B), and the amine-containing sensors showed a visible color change in the presence of acrolein vapors (Figure 3A). Of the amine-containing sensors, the pararosaniline sensors changed from a pink to a purple color, and the 4,4′-azodianiline sensors changed from a yellow to an orange/brown color. Sensor responses (ΔE) were plotted against the mass of the analyte loaded into the test chamber, and the resulting calibration curves are shown for acrolein and acetic acid in Figure 3C,D, respectively. The array showed increased responses to increasing amounts of each analyte (up to approximately 10 mg) before reaching saturation, as evidenced by the plateau in each graph shown. The carbonyl sensors (7−16) showed a wide response range to acrolein (ΔE up to approx. 700), while sensors 1−6 had a more moderate range (ΔE up to approx. 200) in response to acetic acid. The addition of *p*-toluenesulfonic or sulfuric acid to pararosaniline and 4,4′-azodianiline sensors has been shown to enhance sensor response to carbonyl compounds.[35] Individual responses (ΔE) for sensors 7−16 were plotted against the mass of acrolein loaded into the test chamber, and the resulting calibration curves are shown in Figure S10, where the enhancement effect can be observed. Overall, the results shown in Figure 3 indicate that the color change of the sensor array responded proportionally to the lower concentrations of acrolein and acetic acid before reaching a saturation point, meaning that the CSA could be employed for analysis of aldehydes and acids over this range of concentrations and even for semi-quantitative analysis using the corresponding fitting curves between color change (ΔE) and analyte concentration.

Application of Sensor Array to the Analysis of VOCs from Heated Cooking Oils. Deterioration of cooking oils during heating is accompanied by the generation of volatile fatty acids and large amounts of aldehydes as secondary oxidation products.[11] The CSA was tested against the volatile emissions from heated cooking oils (sunflower, rapeseed, olive, and groundnut oils). Figure 4A−D shows the resultant sensor difference maps where distinctive response patterns unique to

https://dx.doi.org/10.1021/acsomega.0c05667
ACS Omega 2021, 6, 7394−7401

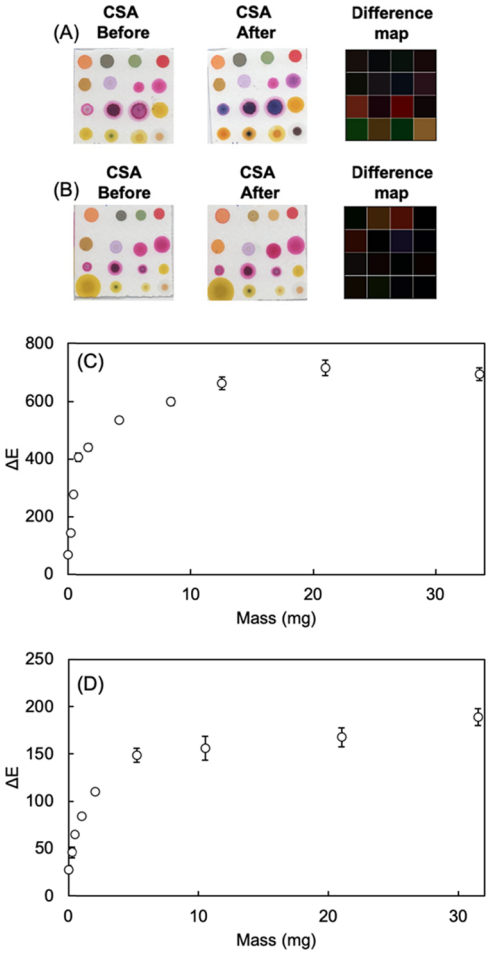

Figure 3. Images of sensor array taken before and after exposure to (A) acrolein and (B) acetic acid vapors. Color difference maps of the array were calculated based on sensor color change in response to standard vapors. Graphs show Δ*E* (Euclidean distance) for carbonyl sensors to increasing amounts of (C) acrolein and pH sensors to increasing amounts of (D) acetic acid. Error bars represent the standard deviation of triplicates.

each cooking oil under investigation are evident. Color changes were observed for the acid sensors, as a response to the volatile fatty acid emissions from the oils. The greatest color changes were observed for the amine-containing dyes reacting with volatile aldehydes, which form a major component of cooking oil emissions.[12] HCA was performed on the dataset (comprising ΔE values), and the dendrogram shown in Figure S11 highlights the capability of the CSA to discriminate between emissions from the four cooking oils and ambient air.

Figure 4E shows the total response for the pH and amine-containing sensors after exposure to cooking oil emissions. Both groups of sensors underwent a color change after exposure to emissions from all four cooking oils suggesting the presence of volatile acids, aldehydes, and ketones. The amine-containing sensors underwent the greatest color change in the presence of sunflower oil followed by rapeseed oil, olive oil, and finally groundnut oil. These results suggest that heating sunflower oil produced higher levels of volatile aldehydes compared to the other cooking oils under investigation. The fatty acid composition of an oil is an important factor influencing the nature and amount of volatile emissions produced during frying,[11] and sunflower oil has been shown to produce very high aldehyde emissions when heated compared to oils with a lower unsaturated fatty acid content (e.g., rapeseed oil) regardless of the cooking method or food type.[2] Fullana et al. saw a similar trend in aldehyde emissions from canola and olive oils when frying at temperatures <180 °C.[36] The acid sensors also underwent the greatest color change in the presence of sunflower oil (Figure 4A), which may have been influenced both by primary volatile fatty acid emissions and secondary decomposition of volatile aldehydes to form volatile acids.[37]

Emissions from the heated cooking oils were also investigated using solid-phase microextraction GC−MS (SPME GC−MS). A total of 33 aldehydes, ketones, and acids were identified based on matches with the mass spectral library and retention index matching. The total chromatographic peak areas for aldehydes, ketones, and acids in cooking oil emissions are shown in Figure S12, where the emissions for each oil appear similar to those characterized by the sensor array (Figure 4E). Sunflower oil produced the highest levels of volatile aldehydes and ketones followed by rapeseed, olive, and groundnut oils.

The GC−MS results are further summarized in a heatmap shown in Figure S13. A total of 19 aldehydes were identified, and they can be categorized into three groups: alkanals

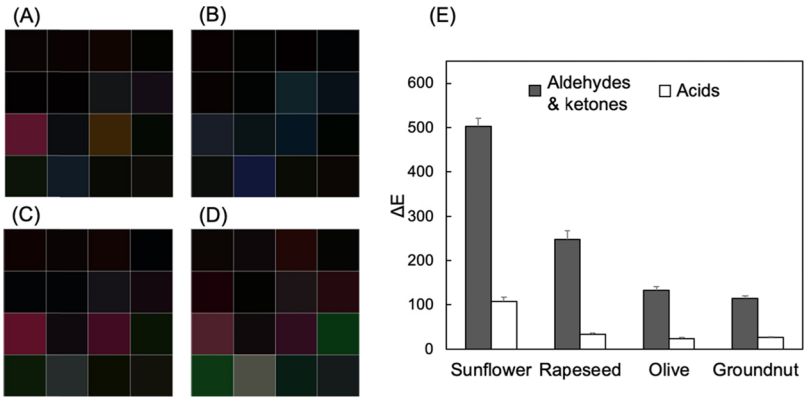

Figure 4. Difference maps showing the change in color (ΔRGB) for each sensor on the array after exposure to (A) rapeseed oil, (B) olive oil, (C) groundnut oil, and (D) sunflower oil; (E) quantification of total volatile aldehydes, ketones, and acids in cooking emissions using CSAs (the *y* axis shows the sum of Δ*E* values for sensors 1−6 (white marker) and sensors 7−16 (gray marker); error bars represent standard deviation of triplicates).

https://dx.doi.org/10.1021/acsomega.0c05667
ACS Omega 2021, 6, 7394−7401

(hexanal, heptanal, octanal, nonanal, decanal, undecanal, dodecanal, and tetradecanal), alkenals (2-ethylacrolein, 2-butenal, 2-hexenal, 2-heptenal, 2-octenal, 2-nonenal, 2-decenal, and 2-undecenal), and alkadienals (2,4-heptadienal, 2,4-nonadienal, and 2,4-decadienal). In addition, there were 10 acids (hexanoic acid, heptanoic acid, octanoic acid, nonanoic acid, decanoic acid, dodecanoic acid, hexadecenoic acid, tetradecanoic acid, 3-heptenoic acid, and 9-hexadecenoic acid) and 4 ketones (1-octen-3-one, 3-nonen-2-one, 2-pentadecanone, and 6,10-dimethyl-5,9-undecadien-2-one/geranyl acetone) identified in the samples. The fatty acid composition of an oil is a key factor influencing the nature and amount of volatile emissions produced during frying.[11] Linoleic acid is an important precursor of volatile aldehydes including hexanal, heptanal, 2-heptenal, 2-nonenal, and 2,4-decadienal[11,38] The highest amounts of these aldehydes were observed in emissions from sunflower oil (Figure S13) due to the oil's high linoleic acid content.[39] Several aldehydes produced from oleic acid (e.g., octanal and decanal) were present in higher amounts in olive and groundnut oils, which have a higher content of oleic acid compared to sunflower and rapeseed oils.[39] The higher recovery of 2,4-heptadienal and 2-butenal from rapeseed oil could also be due to its higher content of linolenic acid compared to sunflower oil.[11,39] Using oils lower in linoleic acid can reduce the emission of volatile aldehydes in cooking oil fumes, especially long chain aldehydes like hexanal and *trans*, *trans*-2,4-decadienal.[2] This reduction was evident in the present study (Figure S13) where rapeseed, olive, and groundnut oils had lower emissions of these compounds compared to sunflower oil.

The total chromatographic peak areas for aldehydes, ketones, and acids in cooking oil emissions were plotted as a function of sensor response, as shown in Figure 5. Linear regression was performed on the data, and a strong positive correlation between the sensor response and peak area of volatile aldehydes, ketones, and acids was observed (R^2 = 0.965). This result serves to validate the quantitative performance of the sensor array, further supporting the suitability of this approach for measurement of VOC emissions from cooking. This CSA holds great potential as a low-cost, easy-to-visualize tool to assist with providing quantitative and qualitative information on potential emission exposures from cooking.

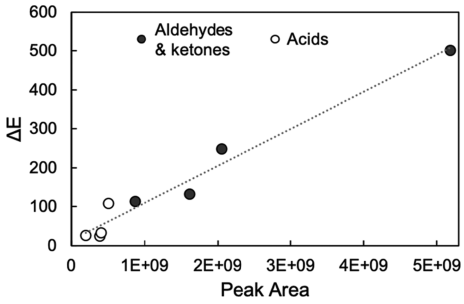

Figure 5. Sensor response versus peak area of volatile aldehydes, ketones, and acids (analyzed by SPME GC−MS) from heated cooking oil emissions (R^2 = 0.965). The *y* axis shows the sum of Δ*E* values for sensors 1−6 (white marker) and sensors 7−16 (black marker). (Data points represent average values, *n* = 3 for each data point).

CONCLUSIONS

The present study aimed to develop a CSA as a new method to characterize VOC emissions from heated cooking oils used in cooking in the domestic setting. The CSA was composed of pH indicators and aniline dyes from classical spot tests, which enabled molecular recognition of a variety of aldehydes, ketones, and acids as demonstrated by hierarchical cluster and principal component analyses. The CSAs were employed for differentiation of VOC emissions from cooking oils (sunflower, rapeseed, olive, and groundnut oils). CSA results were compared to SPME GC−MS analysis results of cooking oil emissions, and a strong positive correlation was observed between the two methods, validating the sensor performance and highlighting the suitability of the sensor array for measurement of VOC emissions from cooking. In terms of limitations to the present study, certain results may have been influenced by low precision in the method (e.g., inter-SPME fiber variability for GC−MS analysis) or interexperiment variability (e.g., small changes in ambient temperature or humidity during sampling). Moreover, only reliably identified VOCs from cooking were reported herein; thus, a number of potentially relevant compounds were not considered in the context of sensor response. Future work will focus on testing the CSA in indoor environments towards understanding the impact of occupant activities like cooking on indoor air pollution. Expansion of the sensor array will also be investigated to target additional compound classes of interest. Overall, the CSA approach has proven to be advantageous for discrimination of the complex mixtures of VOCs generated through cooking and was validated by GC−MS. It holds great potential as a low-cost, easy-to-visualize tool to assist with improving air quality in the cooking environment.

EXPERIMENTAL SECTION

Materials. Thymol blue sodium salt (ACS reagent), bromophenol blue (ACS reagent), bromocresol green (ACS reagent), methyl red (Fluka Analytical), nitrazine yellow (indicator grade), methyltriethoxysilane (technical grade, 90%), triethoxy(octyl)silane (≥97.5%), 2-methoxyethanol (anhydrous 99.8%), propylene glycol methyl ether acetate (Reagent Plus ≥99.5%), polyethylene glycol *tert*-octylphenyl ether (laboratory grade), pararosaniline base, *N*,*N*-dimethyl-4,4′-azodianiline (ACROS Organics, 95%), *p*-toluenesulfonic acid (TsOH), and sulfuric acid (H_2SO_4) were purchased from Sigma-Aldrich (Arklow, Co. Wicklow, Ireland). Analytical standards were also purchased from Sigma-Aldrich, Ireland. Substrates (TLC plates, Polygram CEL 300) were obtained from Machery-Nagel GmbH (Düren, Germany). Water used was high-purity Milli-Q water (Millipore >18MΩcm). SPME fibers comprising 50/30 μm divinylbenzene/carboxen/polydimethylsiloxane (DVB/Car/PDMS) StableFlex (2 cm) assemblies were purchased from Supelco Corp. (Bellefonte, PA, USA). Fibers were conditioned at 250 °C for 25 min before use each day. The cooking oils (rapeseed oil, groundnut oil, extra virgin olive oil, and sunflower oil) were purchased from a local supermarket in Santry, Dublin 9, Ireland.

Preparation of Sensors. Optimized sensor formulations were prepared according to a previously published protocol,[35] and the final array contained 16 sensor spots, as shown in Figure S1. Each pH indicator (4 mg) was dissolved in 1 mL of a sol gel, which was prepared by mixing silane precursors (methyltriethoxysilane and triethoxy(octyl)silane) with 2-

https://dx.doi.org/10.1021/acsomega.0c05667
ACS Omega 2021, 6, 7394−7401

methoxyethanol, propylene glycol methyl ether acetate, deionized, water and a catalyst (0.1 M hydrochloric acid) in a molar ratio of 1:1:25:10:70:0.05. The mixture was stirred overnight at room temperature to yield a sol gel. Pararosaniline and *N,N*-dimethyl-4,4′-azodianiline dyes were mixed with one of two acids (sulfuric or p-toluenesulfonic acid) in different molar ratios and dissolved in a plasticizer (polyethylene glycol *tert*-octylphenyl ether). The dyes and formulations used in each sensor spot are listed in Table S1. Sensor arrays were created by printing the 16 formulations on substrates using micropipettes, constructing a 4 × 4 sensor array. Sensor arrays were dried under vacuum overnight and then stored under vacuum until use.

Image Analysis. A digital scanner (Epson XP-322) was used to capture images (600 DPI resolution) of sensor arrays before and after exposure to volatile analytes. Red (R), green (G), and blue (B) values were measured for each sensor spot before and after exposure using Digital Colour Meter software (Version 5.13, Apple Inc.) where averaged RGB values were recorded from a 25-pixel area on each sensor spot. Color change, or ΔRGB, was calculated by taking the difference of the R, G, and B components before and after exposure. The response for each sensor was calculated using the Euclidean distance (ΔE) formula shown in eq 1:

$$\Delta E = \sqrt{(\Delta R^2 + \Delta G^2 + \Delta B^2)} \quad (1)$$

where ΔR is the difference between the red component in the images collected before and after exposure. Digital images of sensor arrays showing ΔRGB were produced using Microsoft Powerpoint (Version 16.22) to generate difference maps indicating color change of the sensor spots and their response to a particular analyte or sample.

Characterization of Colorimetric Sensor Response to Standard Vapors. Standard analytes and colorimetric sensors were loaded into glass chambers (1.8 L volume) for measurement of colorimetric response. To investigate sensor response to standard vapors, 25 mg of each liquid analyte was dropped onto filter paper, which was suspended at the top of the test chamber. CSAs were placed at the bottom of the chamber to detect analyte vapors. A diagram of the experimental set-up is shown in Figure S2. The chamber was closed, and sensor response was recorded after a 2 h period inside the chamber, using a digital scanner to take an image of the sensor array. Experiments were repeated in triplicate with separate sensor arrays. Control measurements were also performed in the test chambers in the absence of any analytes. Sensor response under different conditions of humidity was investigated using saturated salt solutions of sodium chloride and potassium chloride. The sensor array was also applied to a quantitative analysis of different concentrations of a single aldehyde (acrolein vapor, 0.11−18.6 mg/L) and acid (acetic acid vapor, 0.14−17.5 mg/L). Responses to acetic acid were calculated as the sum of ΔE values for sensors 1−6 (listed in Table S1), and responses to acrolein were calculated as the sum of ΔE values for sensors 7−16 (listed in Table S1). Data processing and analysis were performed using Microsoft Excel and R Studio (version 1.2.5033). R packages ggplot2, factoextra, FactoMineR, and pheatmap were used for data analysis and generation of figures. Euclidean distance was used as the similarity measure method, and Ward's method was used as the linkage method for hierarchical cluster analysis.

Characterization of Colorimetric Sensor Response to Cooking Emissions. Sensor response to emissions produced from heated cooking oils (sunflower oil, rapeseed oil, groundnut oil, and extra virgin olive oil) was investigated. Each oil was heated inside a 2 L glass chamber on a hot plate. Once the temperature of the oil reached 100 °C, CSAs were suspended at the top of the chamber to detect emissions. After a 30 min exposure period, sensor response was recorded using a digital scanner to take an image and ΔRGB values were calculated as outlined above. The exposure time employed for this study was 30 min as it represented a typical time period for cooking activity. SPME fibers were also hung at the top of the chamber to capture cooking emissions during the 30 min experiments. A diagram of the experimental set-up is shown in Figure S3. SPME fibers were analyzed immediately afterward by GC−MS. Experiments were performed in triplicate.

Gas Chromatography−Mass Spectrometry. SPME samples were thermally desorbed in an SPME inlet liner (Supelco, Bellefonte, PA, USA) in the injector of an Agilent 6890 gas chromatograph equipped with a Merlin Microseal (Merlin Instrument Co. Newark, DE, USA). Sample desorption was performed at 250 °C for 2 min, and the injector was operated in splitless mode. The GC system was connected to an Agilent 5973 mass selective detector. The separation column was an SLB-5 ms (30 m × 0.25 mm × 0.25 μm d_f Supelco, Bellefonte, PA, USA), and the helium carrier gas was maintained at a constant flow rate of 1 mL min^{-1}. The GC oven temperature was set to 40 °C for 5 min, after which the oven was programmed at a rate of 10 °C/min to 270 °C with a hold for 2 min. MS was operated at a scan rate of 3.94 s^{-1} and a range of 35−400 *m/z*. The ion source temperature was maintained at 230 °C, and an ionizing energy of 70 eV was used. Data processing and analysis were performed using Agilent GC/MSD ChemStation and OpenChrom software. Compound identification was performed using the National Institute of Standards and Technology library (2005) to >80% match factor and was supported by retention index (RI) matching (tolerance of ≤10 RI units) for which a standard mixture of saturated alkanes was used (C_7-C_{30} Sigma Aldrich, Ireland). Tabulated chromatographic peak areas of reliably identified compounds were imported into Microsoft Excel and R Studio for data analysis. For generation of a heat map showing GC−MS data, peak area values were scaled for each compound using eq 2,

$$\text{scaled value} = \frac{(x - \mu)}{s} \quad (2)$$

where x is the peak area in a sample, μ is the mean peak area across all samples, and s is the standard deviation of peak areas across all samples.

■ ASSOCIATED CONTENT

Supporting Information

The Supporting Information is available free of charge at https://pubs.acs.org/doi/10.1021/acsomega.0c05667.

Composition of the colorimetric sensor array; colorimetric sensor array image, diagram showing the experimental setup for testing sensor response to standard vapors; diagram showing the experimental setup for testing sensor response to cooking emissions; images of the sensor array before and after exposure to standard vapors; difference maps showing color change

https://dx.doi.org/10.1021/acsomega.0c05667
ACS Omega 2021, 6, 7394−7401

under different conditions of humidity; scores plot from principal component analysis on sensor responses to standard analytes; contributions of individual sensors to principal component 1; contributions of individual sensors to principal component 2; correlation plot from principal component analysis; graphs showing carbonyl sensor response to increasing amounts of acrolein; dendrogram from hierarchical clustering analysis of sensor response to heated cooking oil emissions; peak area of aldehydes, ketones, and acids recovered from heated cooking oils by solid-phase microextraction GC−MS; heat map showing compounds recovered from cooking oil emissions by solid-phase microextraction GC−MS (PDF)

AUTHOR INFORMATION

Corresponding Authors

Emer Duffy − *INSIGHT SFI Research Centre for Data Analytics, National Centre for Sensor Research, School of Chemical Sciences, Dublin City University, Dublin 9, Ireland*; Email: emer.duffy25@mail.dcu.ie

Aoife Morrin − *INSIGHT SFI Research Centre for Data Analytics, National Centre for Sensor Research, School of Chemical Sciences, Dublin City University, Dublin 9, Ireland*; orcid.org/0000-0002-3031-4794; Email: aoife.morrin@dcu.ie

Author

Emme Cauven − *School of Natural Science, Fontys University of Applied Sciences, 5612AP Eindhoven, The Netherlands*

Complete contact information is available at: https://pubs.acs.org/10.1021/acsomega.0c05667

Notes

The authors declare no competing financial interest.

ACKNOWLEDGMENTS

This research was supported by funding from the European Union's Horizon 2020 Research and Innovation Programme under the Marie Skłodowska-Curie grant agreement number 796289 and Science Foundation Ireland (SFI) under Grant Number SFI/12/RC/2289_P2, co-funded by the European Regional Development Fund. The authors would also like to thank Mary Ross for technical support.

REFERENCES

(1) Abdullahi, K. L.; Delgado-Saborit, J. M.; Harrison, R. M. Emissions and Indoor Concentrations of Particulate Matter and Its Specific Chemical Components from Cooking: A Review. *Atmos. Environ.* **2013**, *71*, 260−294.

(2) Peng, C.-Y.; Lan, C.-H.; Lin, P.-C.; Kuo, Y.-C. Effects of Cooking Method, Cooking Oil, and Food Type on Aldehyde Emissions in Cooking Oil Fumes. *J. Hazard. Mater.* **2017**, *324*, 160−167.

(3) He, C.; Morawska, L.; Hitchins, J.; Gilbert, D. Contribution from Indoor Sources to Particle Number and Mass Concentrations in Residential Houses. *Atmos. Environ.* **2004**, *38*, 3405−3415.

(4) Lee, S. C.; Li, W. M.; Chan, L. Y. Indoor Air Quality at Restaurants with Different Styles of Cooking in Metropolitan Hong Kong. *Sci. Total Environ.* **2001**, *279*, 181−193.

(5) Buonanno, G.; Morawska, L.; Stabile, L. Particle Emission Factors during Cooking Activities. *Atmos. Environ.* **2009**, *43*, 3235−3242.

(6) Shields, P. G.; Xu, G. X.; Blot, W. J.; Fraumeni, J. F.; Trivers, G. E.; Pellizzari, E. D.; Qu, Y. H.; Gao, Y. T.; Harris, C. C. Mutagens from Heated Chinese and U.S. Cooking Oils. *J. Natl. Cancer Inst.* **1995**, *87*, 836−841.

(7) Thiébaud, H. P.; Knize, M. G.; Kuzmicky, P. A.; Hsieh, D. P.; Felton, J. S. Airborne Mutagens Produced by Frying Beef, Pork and a Soy-Based Food. *Food Chem. Toxicol.* **1995**, *33*, 821−828.

(8) Chiang, T. A.; Wu, P. F.; Wang, L. F.; Lee, H.; Lee, C. H.; Ko, Y. C. Mutagenicity and Polycyclic Aromatic Hydrocarbon Content of Fumes from Heated Cooking Oils Produced in Taiwan. *Mutat. Res.* **1997**, *381*, 157−161.

(9) Qu, Y. H.; Xu, G. X.; Zhou, J. Z.; Chen, T. D.; Zhu, L. F.; Shields, P. G.; Wang, H. W.; Gao, Y. T. Genotoxicity of Heated Cooking Oil Vapors. *Mutat. Res.* **1992**, *298*, 105−111.

(10) Agents Classified by the IARC Monographs, Volumes 1-125 - IARC Monographs on the Identification of Carcinogenic Hazards to Humans https://monographs.iarc.fr/agents-classified-by-the-iarc/ (accessed May 18, 2020).

(11) Katsuta, I.; Shimizu, M.; Yamaguchi, T.; Nakajima, Y. Emission of Volatile Aldehydes from DAG-Rich and TAG-Rich Oils with Different Degrees of Unsaturation During Deep-Frying. *J. Am. Oil Chem. Soc.* **2008**, *85*, 513−519.

(12) Katragadda, H. R.; Fullana, A.; Sidhu, S.; Carbonell-Barrachina, Á. A. Emissions of Volatile Aldehydes from Heated Cooking Oils. *Food Chem.* **2010**, *120*, 59−65.

(13) Yu, I. T. S.; Chiu, Y.-L.; Au, J. S. K.; Wong, T.-W.; Tang, J.-L. Dose-Response Relationship between Cooking Fumes Exposures and Lung Cancer among Chinese Nonsmoking Women. *Cancer Res.* **2006**, *66*, 4961−4967.

(14) Seaman, V. Y.; Bennett, D. H.; Cahill, T. M. Indoor Acrolein Emission and Decay Rates Resulting from Domestic Cooking Events. *Atmos. Environ.* **2009**, *43*, 6199−6204.

(15) Young, S.-C.; Chang, L. W.; Lee, H.-L.; Tsai, L.-H.; Liu, Y.-C.; Lin, P. DNA Damages Induced by Trans, Trans-2,4-Decadienal (Tt-DDE), a Component of Cooking Oil Fume, in Human Bronchial Epithelial Cells. *Environ. Mol. Mutagen.* **2010**, *51*, 315−321.

(16) Chang, Y.-C.; Lin, P. Trans, Trans-2,4-Decadienal Induced Cell Proliferation via P27 Pathway in Human Bronchial Epithelial Cells. *Toxicol. Appl. Pharmacol.* **2008**, *228*, 76−83.

(17) Tang, X.; Misztal, P. K.; Nazaroff, W. W.; Goldstein, A. H. Volatile Organic Compound Emissions from Humans Indoors. *Environ. Sci. Technol.* **2016**, *50*, 12686−12694.

(18) Farmer, D. K.; Vance, M. E.; Abbatt, J. P. D.; Abeleira, A.; Alves, M. R.; Arata, C.; Boedicker, E.; Bourne, S.; Cardoso-Saldaña, F.; Corsi, R.; DeCarlo, P. F.; Goldstein, A. H.; Grassian, V. H.; Ruiz, L. H.; Jimenez, J. L.; Kahan, T. F.; Katz, E. F.; Mattila, J. M.; Nazaroff, W. W.; Novoselac, A.; O'Brien, R. E.; Or, V. W.; Patel, S.; Sankhyan, S.; Stevens, P. S.; Tian, Y.; Wade, M.; Wang, C.; Zhou, S.; Zhou, Y. Overview of HOMEChem: House Observations of Microbial and Environmental Chemistry. *Environ. Sci.: Processes Impacts* **2019**, *21*, 1280−1300.

(19) Zhu, X.; Wang, K.; Zhu, J.; Koga, M. Analysis of Cooking Oil Fumes by Ultraviolet Spectrometry and Gas Chromatography−Mass Spectrometry. *J. Agric. Food Chem.* **2001**, *49*, 4790−4794.

(20) Khot, L. R.; Panigrahi, S.; Lin, D. Development and Evaluation of Piezoelectric-Polymer Thin Film Sensors for Low Concentration Detection of Volatile Organic Compounds Related to Food Safety Applications. *Sens. Actuators B: Chem.* **2011**, *153*, 1−10.

(21) Lipatov, A.; Varezhnikov, A.; Wilson, P.; Sysoev, V.; Kolmakov, A.; Sinitskii, A. Highly Selective Gas Sensor Arrays Based on Thermally Reduced Graphene Oxide. *Nanoscale* **2013**, *5*, 5426−5434.

(22) Echeverría, J. C.; Faustini, M.; Garrido, J. J. Effects of the Porous Texture and Surface Chemistry of Silica Xerogels on the Sensitivity of Fiber-Optic Sensors toward VOCs. *Sens. Actuators B: Chem.* **2016**, *222*, 1166−1174.

(23) Liu, D.; Kumar, R.; Wei, F.; Han, W.; Mallik, A. K.; Yuan, J.; Wan, S.; He, X.; Kang, Z.; Li, F.; Yu, C.; Farrell, G.; Semenova, Y.; Wu, Q. High Sensitivity Optical Fiber Sensors for Simultaneous Measurement of Methanol and Ethanol. *Sens. Actuators B: Chem.* **2018**, *271*, 1−8.

(24) Janzen, M. C.; Ponder, J. B.; Bailey, D. P.; Ingison, C. K.; Suslick, K. S. Colorimetric Sensor Arrays for Volatile Organic Compounds. *Anal. Chem.* **2006**, *78*, 3591−3600.
(25) Park, D.-H.; Heo, J.-M.; Jeong, W.; Yoo, Y. H.; Park, B. J.; Kim, J.-M. Smartphone-Based VOC Sensor Using Colorimetric Polydiacetylenes. *ACS Appl. Mater. Interfaces* **2018**, *10*, 5014−5021.
(26) Diehl, K. L.; Anslyn, E. V. Array Sensing Using Optical Methods for Detection of Chemical and Biological Hazards. *Chem. Soc. Rev.* **2013**, *42*, 8596−8611.
(27) Rakow, N. A.; Suslick, K. S. A Colorimetric Sensor Array for Odour Visualization. *Nature* **2000**, *406*, 710−713.
(28) Azzouz, A.; Vikrant, K.; Kim, K.-H.; Ballesteros, E.; Rhadfi, T.; Malik, A. K. Advances in Colorimetric and Optical Sensing for Gaseous Volatile Organic Compounds. *TrAC Trends Anal. Chem.* **2019**, *118*, 502−516.
(29) Li, J.; Hou, C.; Huo, D.; Yang, M.; Fa, H.; Yang, P. Development of a Colorimetric Sensor Array for the Discrimination of Aldehydes. *Sens. Actuators B: Chem.* **2014**, *196*, 10−17.
(30) Piriya, V. S. A.; Joseph, P.; Daniel, S. C. G. K.; Lakshmanan, S.; Kinoshita, T.; Muthusamy, S. Colorimetric Sensors for Rapid Detection of Various Analytes. *Mater. Sci. Eng.: C* **2017**, *78*, 1231−1245.
(31) Davidson, C. E.; Dixon, M. M.; Williams, B. R.; Kilper, G. K.; Lim, S. H.; Martino, R. A.; Rhodes, P.; Hulet, M. S.; Miles, R. W.; Samuels, A. C.; Emanuel, P. A.; Miklos, A. E. Detection of Chemical Warfare Agents by Colorimetric Sensor Arrays. *ACS Sens.* **2020**, *5*, 1102−1109.
(32) Hoang, A. T.; Cho, Y. B.; Kim, Y. S. A Strip Array of Colorimetric Sensors for Visualizing a Concentration Level of Gaseous Analytes with Basicity. *Sens. Actuators B: Chem.* **2017**, *251*, 1089−1095.
(33) Lim, S. H.; Feng, L.; Kemling, J. W.; Musto, C. J.; Suslick, K. S. An Optoelectronic Nose for the Detection of Toxic Gases. *Nat. Chem.* **2009**, *1*, 562−567.
(34) Soga, T.; Jimbo, Y.; Suzuki, K.; Citterio, D. Inkjet-Printed Paper-Based Colorimetric Sensor Array for the Discrimination of Volatile Primary Amines. *Anal. Chem.* **2013**, *85*, 8973−8978.
(35) Li, Z.; Fang, M.; LaGasse, M. K.; Askim, J. R.; Suslick, K. S. Colorimetric Recognition of Aldehydes and Ketones. *Angew. Chem., Int. Ed. Engl.* **2017**, *56*, 9860−9863.
(36) Fullana, A.; Carbonell-Barrachina, Á. A.; Sidhu, S. Volatile Aldehyde Emissions from Heated Cooking Oils. *J. Sci. Food Agric.* **2004**, *84*, 2015−2021.
(37) Przybylski, R.; Eskin, N. A. M. Methods to Measure Volatile Compounds and the Flavor Significance of Volatile Compounds. In *Methods to Access Quality and Stability of Oils and Fat-Containing Foods*.; Warner, K.; Eskin, N.A.M., Ed.; AOCS Press: Illinois, 1995; 107−133.
(38) Fullana, A.; Carbonell-Barrachina, A. A.; Sidhu, S. Comparison of Volatile Aldehydes Present in the Cooking Fumes of Extra Virgin Olive, Olive, and Canola Oils. *J. Agric. Food Chem.* **2004**, *52*, 5207−5214.
(39) Orsavova, J.; Misurcova, L.; Ambrozova, J. V.; Vicha, R.; Mlcek, J. Fatty Acids Composition of Vegetable Oils and Its Contribution to Dietary Energy Intake and Dependence of Cardiovascular Mortality on Dietary Intake of Fatty Acids. *Int. J. Mol. Sci.* **2015**, *16*, 12871−12890.

https://dx.doi.org/10.1021/acsomega.0c05667
ACS Omega 2021, 6, 7394−7401